Prepublished copy

Nature Environment & Pollution Technology

This is a peer-reviewed prepublished version of the paper

Green Synthesis of Semiconductor Nanocomposite (O-ZnO) Using Onion Peels Extract For Degradation Of Organic Material

Nabaa A. Al-Wahab[1*], Rasha A. Al-Husseiny[2]

[1,2] Water resources management Engineering Dep., College of Engineering, Al Qasim Green University,51013, Babylon, Iraq

[1]nabaaabedalwahab@wrec.uoqasim.edu.iq

[2]rasha83@wrec.uoqasim.edu.iq

* Corresponding Author: Nabaa A. Al-Wahab; email: nabaaabedalwahab@wrec.uoqasim.edu.iq

https://orcid.org/0000-0001-9228-0289

Abstract:

The overuse of pharmaceuticals in recent years and the subsequent discharge of pharmaceutical waste, liquid waste, and harmful organic pollutants into the aquatic environment are important issues that should be seriously addressed. Therefore, this work presented an economical, environmentally sustainable, and simple method for producing zinc oxide nanocomposite using onion peels extract (OPE) and using this nanocomposite (O-ZnO) for organic pollutant removal as cefixime (Cfx) from aqueous solution using an advanced oxidation process. The synthesized materials in this study were characterized using analytical techniques, including (Brunauer–Emmett–Teller (BET), X-ray diffraction (XRD), field emission scanning electron microscopes (FESEM), and Fourier transform infrared spectroscopy (FTIR). The analysis showed that the surface area of onion peels extract (OPE), ZnONPs without OPE, and ZnO with OPE (O-ZnO) were 4.22, 30.1, and 49.3 m2/g, respectively. The findings indicated that the cefixime elimination efficiency of the O-ZnO nanocomposite attained 94%. Under the best operational conditions of pH (4), the dosage of O-ZnO (0.4 mg/L), Cfx concentration was (10 mg/L) with optimum contact time 120min. The kinetic degradation rate of (Cfx) adhered to the pseudo-first-order equation with an R^2 value of 0.9682, giving a constant degradation rate of 0.03 1/min.

Key Words	Photocatalytic; Green synthesis; Zinc oxide (ZnO); Onion peel extract (OPE); Cefixime (Cfx).
DOI	https://doi.org/10.46488/NEPT.2025.v24i03.D1747 (DOI will be active only after the final publication of the paper)
Citation of the Paper	Nabaa A. Al-Wahab, Rasha A. Al-Husseiny, 2025. Green Synthesis of Semiconductor Nanocomposite (O-ZnO) Using Onion Peels Extract For Degradation Of Organic Material. *Nature Environment and Pollution Technology*, 24(3), D1747. https://doi.org/10.46488/NEPT.2025.v24i03.D1747

1. INTRODUCTION:

The daily activities of humans, factories, and other sources have recently generated large volumes of wastewater. These sources can produce compounds that are hazardous to the environment and human health, as well as materials that are not biodegradable (Ajiwokewu,2024).

Furthermore, significant harm to sustainable development is caused by the rapidly growing amounts of wastewater containing harmful organic contaminants, which are not biodegradable even in drinking water and are very poisonous(Jabbar, Okab, *et al.* 2023).Emerging contaminants, such as antibiotics, have been found in drinking water, sewage effluent, surface water, and even reclaimed land (Moosavi *et al.* 2019). Cefixime (Cfx) is one of the most commonly used antibiotics. Cefixime can be purchased in white or nearly white powder. Cefixime does not dissolve well in water (Abdullah *et al.* 2022). Additionally, the presence of these substances in water supplies, even at deficient concentrations, strengthens their resistance to bacteria (Widyasari *et al.* 2022). In order to eliminate organic pollutants, several instead of a number of technologies have been used, such as sedimentation, adsorption, solvent extraction, chemical precipitation, conventional biological processes, and electrochemical processes. Unfortunately, these technologies are not cost-effective, the processes are slow, and they need to be controlled in terms of pressure and temperature(Haroon *et al.* 2023). (AOP) has proven effective, affordable, dependable, and promising for eliminating pollutants from aquatic environments(Hidayah, Cahyonugroho and Fauziya, 2023). Among the different AOP techniques, homogeneous and heterogeneous photocatalysis has shown promise in degrading a range of pollutants by employing different catalysts. which uses different kinds of catalysts(Al-husseiny and Ebrahim, 2021). AOP procedures provide low-cost and ecologically friendly treatment options(Al-husseiny *et al.* 2023). nano-semiconductor photocatalysts like TiO2, ZnO, Fe_2O_3, and ZnS have drawn a lot of attention and study due to their great efficiency, non-toxic, low energy consumption, and very efficient in treating sewage(Al-husseiny *et al.* 2023) (Xu and Xu, 2020). (ZnO) is classified as a wide-band gap semiconductor and is a member of the II-VI semiconductor group. ZnO catalysts facilitate the photodegradation of organic compounds through exposure to light. When ZnO is exposed to light with energy higher than its bandgap, electrons in the valence band (VB) are stimulated to move to the conduction band (CB), resulting in the creation of photogenerated electrons in the CB and photogenerated holes in the VB. Biological synthesis is a highly environmentally friendly approach for synthesizing ZnONPs (Nagore et al., 2021), (Roy *et al.* 2022), (Raina et al., 2020). The novelty of this study was synthesize of O-ZnO by using and utilizing from low-cost waste materials to get rid of the problem of solid waste resulting from daily household use or any sources containing quantities of such onion peels.The onion is known to include a variety of phytochemicals, flavonoids, and enzymes that aid in the production of nanoparticles and to achieve sustainability, environmentally friendly, and inexpensive. The natural compounds in onion peel extract promote the generation of hydroxyl radicals (•OH) and superoxide anions (O2•−), which contribute to the breakdown of organic pollutants. These compounds also support the adsorption and catalysis of organic materials, accelerating the degradation process. This work aimed to synthesize nanocomposite O-ZnO utilizing a simple and environmentally friendly method. The reducing and capping agent employed in this process is an extract derived from onion peels waste. The ZnO nanostructures were tested using several spectroscopic and microscopy tools.The photocatalytic effectiveness of ZnO nanostructures was examined when exposed to UV photo-irradiation to degrade organic antibiotic contaminants, specifically cefixime. The synthesized materials were examined using X-ray diffraction,field-emission scanning electron microscopy,

Brunauer-Emmett-Teller, Fourier-Transform infrared spectroscopy, and Barrentt-Joyner-Halenda techniques. Cefixime removal's kinetic model was studied under some of the conditions, such as contact times, pH, O-ZnO dose, and initial cefixime concentrations.

2.Photocatalysis Process:

Photocatalysis is a significant component of advanced oxidation processes (AOPs). These are commonly employed for the elimination of stubborn organic components from industrial and municipal effluent (Thongam & Chaturvedi, 2021). Semiconductor photocatalysis is triggered by the generation of electron-hole pairs following the stimulation of the material's bandgap. When a photocatalyst is exposed to light with energy equivalent to or higher than the band-gap energy, the electrons in the valence band can be stimulated to move to the conduction band, resulting in the creation of a positive hole in the valence band: A photocatalyst, such as zinc oxide (ZnO). The excited electron-hole pairs can undergo recombination, resulting in the dissipation of the input energy as heat, without any chemical alteration. Nevertheless, in the event that the electrons (and holes) go to the surface of the semiconductor without undergoing recombination, they are able to engage in a range of oxidation and reduction reactions with adsorbed substances like water, oxygen, and other organic or inorganic species. The oxidation and reduction reactions serve as the fundamental processes in photocatalytic water/air remediation and photocatalytic hydrogen production, respectively. Fig.(1) shown the Schematic representation of the photocatalytic mechanism of ZnO photocatalyst.

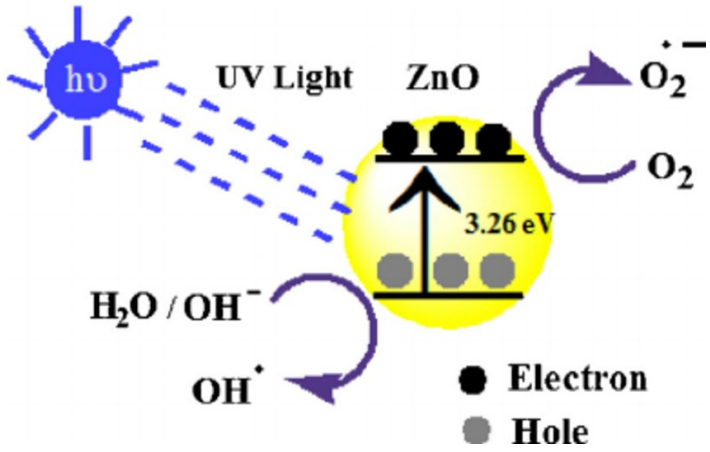

Fig.(1): Schematic representation of the photocatalytic mechanism of ZnO photocatalyst.

3. Comparison with other technologies:

Advanced water treatment technologies have been created to remove pharmaceuticals effectively. Table (1) provide a comprehensive overview of the advantages and disadvantages of various wastewater treatment systems. The typical approach described in Table (1) has significant disadvantages, including partial elimination, large energy requirements, and the production of

hazardous compounds (Al Qarni et al., 2019). Various techniques have been employed to eliminate toxins from polluted water sources. Advanced oxidation processes (AOP) have developed as a potential, effective, affordable, and dependable method for removing contaminants from aquatic environments. Homogeneous and heterogeneous photocatalysis, employing diverse catalysts, has become a feasible approach for breaking down a wide range of contaminants among the many AOP approaches. AOP procedures are classified as cost-effective and ecologically friendly treatment options .

Table (1): Advantages and Disadvantages of Several Wastewater Treatment Technologies**:**

Treatment Technology	Advantage	Disadvantage	References
Coagulation (physical)	-Simplicity and profitability. -Separates many types of particles of water.	- It requires the use of chemical products. -Toxic compounds are transferred to the solid phase	(Wei et al., 2021)
Membrane Bioreactor Technique (biological)	-Membrane filtration ensures water quality is treated regardless of the decantability of the sludge. -High quality and high levels of water disinfection-treated	-High cost of implementation and exploitation. -Accumulation of toxic substances in the bioreactor. Membrane fouling.	(Phoon et al., 2020)
Activated Sludge (biological)	-It is a process that is used in the treatment of wastewater industrial. - It is a process that is used in the treatment of wastewater industrial.	- High costs of design, construction, operation, and maintenance. - High costs of design, construction, operation, and maintenance. -Sludge storage problems residuals.	(Henstra et al., 2007) (M. N. P. F. S. Couto et al., 2010),(J. Huang et al., 2018)
Biological Treatment Process (biological)	- The construction and process operation of these reactors are comparatively simple. -An acceptable and steady pH can be continued without the addition of chemicals	-Pathogens and nutrients are partially removed, and hence post-treatment is needed - The process start-up takes a long time due to the low progress rate of microbes to be active.	(Cecconet et al., 2017); (C. F. Couto et al., 2019) ;(Dogan et al., 2020) .

Constructed Wetlands Process (physical)	-Energy consumption is quite low. - Operational and maintenance costs are low	- A large land area and higher setting time are required. - Many pharmaceuticals cannot be removed completely	(Verlicchi&Zambello, 2014) .

2. MATERIALS AND METHODS:

2.1. Materials:

Various materials were utilized in the experiments, and all chemicals used were of analytical grade. Table (2) lists all the materials used in this work.

Table 2: Sources of materials and chemical formula of starting materials utilized.

Material Name	Chemical Formulas	Supplier
Cefixime	$C_{16}H_{15}N_5O_7S_2$	The general company for the drugs industry (Iraq)
Sodium hydroxide	NaOH	Thomas Baker, India,
Hydrochloric acid	HCl	Thomas Baker, India,
Distilled water	H2O	Lab
Zinc Acetate	Zn $(CH_3CO_2)_2$	Thomas Baker, India,

2.2. SYNTHESIS OF (O-ZnO) NANOCOMPOSITE:

2.2.1. Onion Peels Extract Preparation (OPE):

The onion peels waste obtained from the market for vegetables was thoroughly rinsed several times using two times as much pure water to remove any accompanying microscopic bits of dust. In addition, the item was air-dried at room temperature for two days until complete moisture evaporation occurred. Subsequently, 1 g of the onion peels was introduced into 100 ml of distilled water and subjected to extraction through boiling for 30 minutes. The onion extract was isolated through filtration and utilized to manufacture zinc oxide nanoparticles. Fig. (2) represents the steps of preparing onion peels extract.

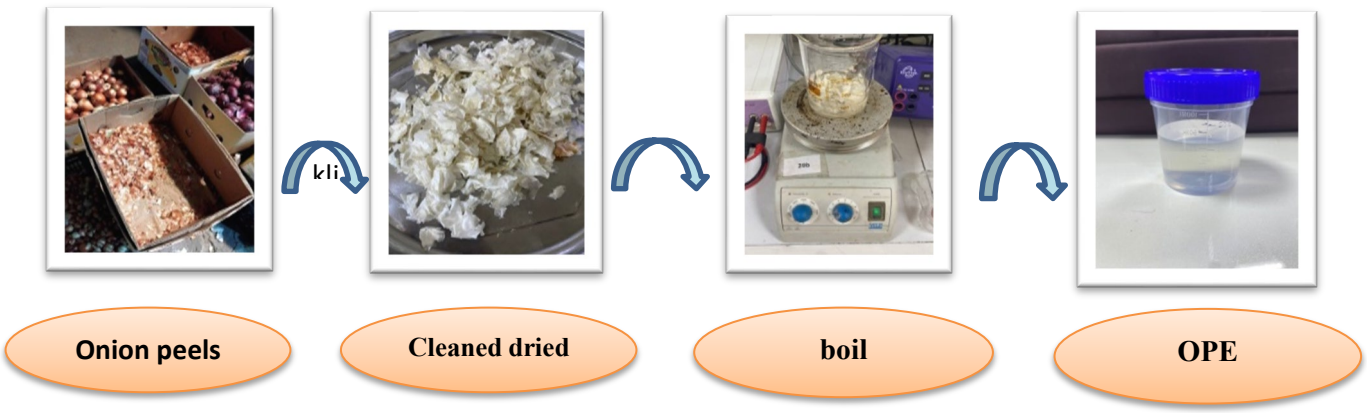

Fig. 2: Steps of preparation of onion peels extract

2.2.2: Synthesis of Nano-composite (O-ZnO):

A magnetic stirrer was used to prepare and hold approximately 50 ml of a 0.2 M solution of zinc acetate (Zn $(CH_3CO_2)_2$). During the experiment, the acidity level of the solution was monitored. kept at 12 by utilizing a 0.2M NaOH solution since the parameters were specified and tuned, and the optimal pH value was determined to be at pH 12 for synthesis. The solution above was value of speed and temperature stirred while approximately 10 mL of onion peel extract solution was included a decrease by drop.(Al-husseiny and Ebrahim, 2022a). Once the incubation duration validated the (O-ZnO) synthesis, the solution was left in stirring conditions for two hours. To distinguish the solution from the residue, the mixture was centrifuged for five minutes at 6000 rpm. While the residue was kept, the solution was decanted. The residue was repeatedly cleaned with D.W. to get rid of any contaminants that might have attached themselves to their surface. After obtaining the residue, it was dried entirely at 70 °C in an oven. Fig.(3) represents the steps of synthesis of (O-ZnO).

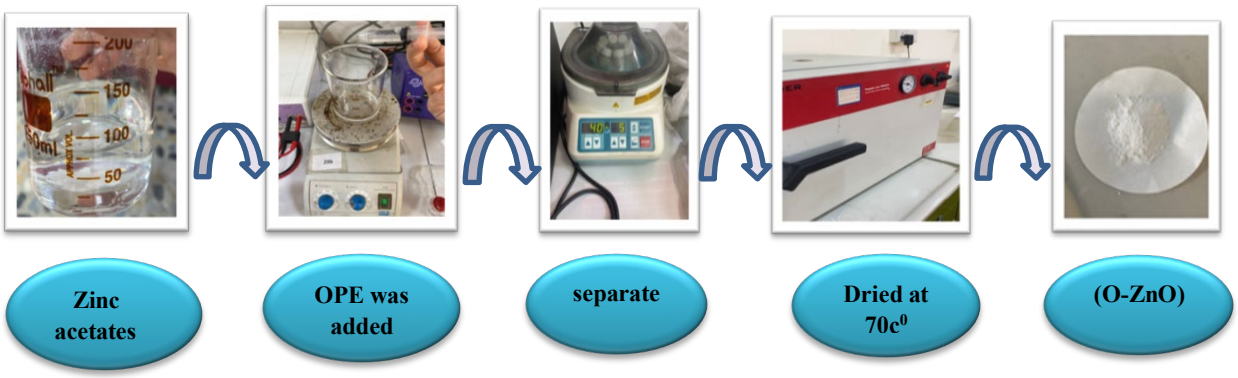

Fig. 3: Steps of synthesis of Nano-composite (O-ZnO).

2.3 Comparison between zinc commercial and nanocomposite (O-ZnO):

In this study, zinc manufactured from onion peel extract was compared with commercial zinc. Fig. (4) compares these materials to choose the optimal removal efficiency for (Cfx). It was noted that the percentage of pollutant removal by (O-ZnO) was 94%, while the pollutant removal by commercial zinc was 49%. This indicates the importance of using peels in the synthesis of zinc, the natural compounds in onion peel extract promote the generation of hydroxyl radicals (•OH) and superoxide anions (O2•−), which contribute to the breakdown of organic pollutants. These

compounds also support the adsorption and catalysis of organic materials, accelerating the degradation process as nanocomposite (O-ZnO) works as a new and inexpensive absorbent material to remove organic pollutants such as (Cfx) due to the higher surface area of the nanocomposite compared to ZnO commercial.

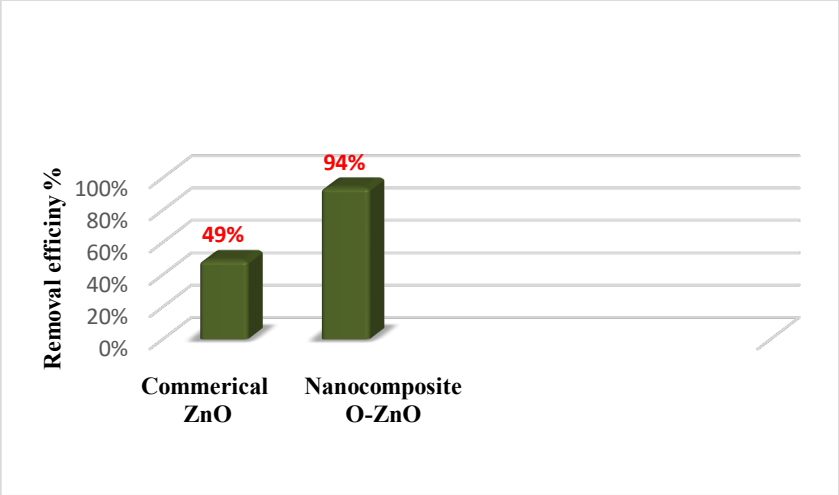

Fig. (4): Comparison between zinc commercial ZnO, and (O-ZnO) nanocomposite**.**

2.4 Photocatalytic Degradation Reaction:

The photocatalytic degradation of cefixime under UV light was examined utilizing green-synthesized ZnO nanoparticles derived from onion peel extract and zinc acetate solution in a batch photocatalytic reactor. Initially, 0.150 g of OPE/ZnO was incorporated into 100 mL of cefixime solution at a starting concentration of 10 mg/L. The solution was thereafter subjected to magnetic stirring in the absence of light for 30 minutes to achieve adsorption equilibrium. Subsequently, the suspensions were exposed to UV light, as illustrated in Fig (5). Following predetermined illumination durations, 5 mL was extracted and centrifuged at 6000 rpm to quantify cefixime concentration. The cefixime concentration was evaluated using UV–vis spectroscopy. (HitachiU2900), with a maximum absorption wavelength of 280 nm.

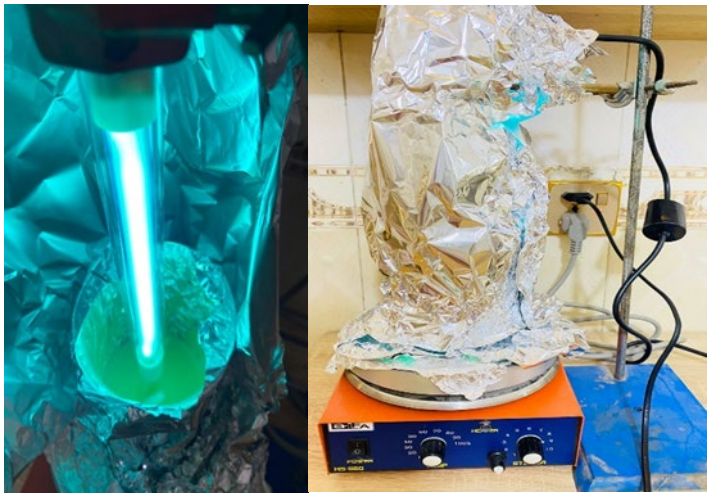

Fig. 5: Batch oxidation system

2.5 Parameters affecting the photocatalytic process.

In this study, the experiments were achieved using changeable parameters in a batch system. as shown in Table (3):

Table 3: Experimental parameters examined in a batch system.

Parameters Range	Ranges
pH	(2-10)
Dosage mg/l	(0.1-0.6)
Initial concentration (ppm (mg/L))	(10-70)
contact time (min)	(30-180)

All experiments were performed at room temperature using a magnetic stirrer. An external magnet was employed to isolate the adsorbent from the solution. A UV spectrophotometer was employed to measure optical properties. The removal effectiveness of Cfx, denoted as R (%), was computed using the eq.1 (Al-husseiny & Ebrahim, 2022).

$$\textbf{Degradation efficiency \%} = \frac{Co - Ct}{Co} * 100\% \quad (1)$$

Where: Co represents the initial concentration, while Ct is the cefixime concentration at a certain reaction time.

3. RESULTS AND DISCUSSIONS:

3.1. Results of characterization:

3.1.1 BET Analysis:

The Brunauer–Emmett–Teller (BET) Analytical techniques were employed to ascertain the surface areas of the adsorbents., and Barrentt-Joyner-Halenda (BJH) Analytical methods were utilised to determine the properties of the pore volumes. and pore sizes of nanomaterials used in this study Presented in Table (4). The analysis showed that the expanse of the surface of onion peel extract (OPE), ZnONPs without OPE, and (O-ZnO) were 4.22, 30.1, and 49.3 m2/g, respectively. (O-ZnO) before removal exhibited the most surface area from OPE and ZnO without OPE. The pore volumes were measured (0.015594, 0.094318, and 0.1284cm3/g) for OPE, ZnO, and (O-ZnO) before removal, respectively, and (O-ZnO) before removal exhibited the greatest pore volume. The pore sizes of OPE, ZnO Without OPE, and (O-ZnO) before removal were (10.61, 6.95, and 4.65 nm), respectively. Increasing BET the surface area of (O-ZnO) before removal, the higher surface area of(O-ZnO). The effectiveness of this adsorbent in removing (Cfx) has been demonstrated through several experiments, highlighting the impact of its elevated pore volume and mean pore diameter of (O-ZnO) before removal compared to OPE, ZnO Without OPE material, It improves the process of adsorption (Cfx) and The accumulation of the substance on the adsorbent is affected by the BET surface area, pore volume, and mean pore diameter, as these are primary parameters affecting adsorption.

Table 4: OPE, ZnO Without OPE, (O-ZnO) before removal, and (O-ZnO) after removal

Characteristics	OPE	ZnO Without OPE	(O-ZnO) before removal	(O-ZnO) after removal
Specific surface area (m^2/g)	4,2217	30,098	49,277	15,391
Total pore volume (cm^3/g)	0,015594	0,094318	0,1284	0,1047
Mesoporous and microporous volume (cm^3/g)	0,9699	6,9151	11,322	3,5361
BJH volume of pores (cm^3/g)	0,014591	0,091405	0,1227	0,1003
BJH surface area of pores (m^2/g)	1,4296	14,724	19,668	17,682
BJH average pore diameter (nm)	10,61	6,95	4,65	10,61

3.1.2 XRD (X-Ray Diffraction) analysis:

X-ray diffraction is an effective method for determining composition of crystalline materials. (XRD) yields information about the sample's crystalline phase, orientation, and network. The crystallinity, analysis of phase, and Particle size crystal were examined using The X-ray diffraction (XRD) technique. Fig. (6- a to d) presents the crystalline structure of the synthesized materials (OPE, ZnO without (O-ZnO), (O-ZnO) before removal of Cfx, and (O-ZnO) after removal Cfx). X-ray diffraction peaks for OPE at (2θ =14.6◦ and 32.5◦) are shown in Fig. (6-a) using a certain code for reference of (96-201-2670) and intensity of (111 and ¯114). The X-ray diffraction (XRD) peaks corresponding to the produced zinc oxide (ZnO) nanoparticles are displayed in Fig.(6-c). XRD pattern of (O-ZnO) shows in fig.(6-b,c)the prominent diffraction peaks observed at the specified diffraction angles (2θ): (32.4◦, 34.2◦, 36.5◦, 47.8◦, 57.6◦, 63◦, 68.14◦, 69.25◦, 72.35◦, and77◦) with reference code of (96-220-4398) and intensity of (220,31-1,22-3, 051,13 -8,15-7, 149,158, and 43-8), respectively. The observations validated the crystalline structure of the nanoparticles as Wurtzite (O-ZnO). Furthermore, the presence of distinct and sharp diffraction peaks suggests a high level of crystallinity in the nanoparticles. The lack of additional diffraction peaks resulting from contaminants and intermediary components demonstrated the exceptional purity of the produced ZnO nanoparticles. Comparable crystalline size dimensions by (Abbes et al., 2022), (Ramesh et al., 2021), (Bekele *et al.* 2021),(Harouni et al., 2019). Utilizing XRD data, it was determined that the peaks are broad, indicating that the crystallites possess sizes within a specific range, and the diameter (D) was computed using Scherrer's formula.

$$D = K\lambda / \beta \cos\theta \qquad (2)$$

Where: The symbol "**K**" represents the Debye Scherrer constant, **"λ"** denotes the X-ray wavelength, "**β**" represents the breadth of the half maximum peak, and **"θ"** signifies the diffraction angle**.** (Drummer et al., 2021). X-ray diffraction data measure the estimated crystalline size of (O-ZnO) The measurement was taken at around 22 nanometers.

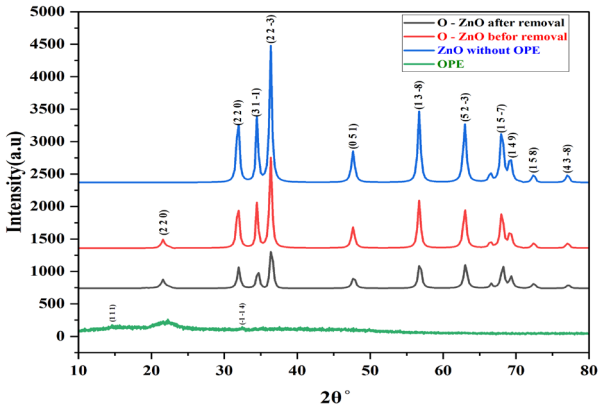

Fig. 6: The X-ray diffraction pattern depicts the structure of (a)OPE (b) ZnO without OPE, (c) (O-ZnO) before removal Cfx, and (d) (O-ZnO) after removal Cfx

3.1.3 Fourier-transform infrared spectroscope (FTIR) of Synthesized materials:

Fig.7 depicts the standard diagram of Fourier Transform Infrared Spectroscopy (FTIR) analysis of Zinc Oxide Nanoparticles (ZnONPs) that were manufactured from onion waste (O-ZnO). The peaks seen at (427.91 and 503.42 cm−1) are ascribed to the ZnO bond and muscular stretching, suggesting the creation of the particles. The band observed at 1036.94 cm-1 in the nanoparticles from the peel is attributed to the presence of an amide group. On the other hand, the sharp and deep band observed at 1632.01 cm−1 is attributed to the stretching of the C = O bond and the existence of a water molecule (−OH) in the nanoparticle. The presence of ambient carbon dioxide on the sample is indicated by a little signal at 2988.16 cm−1. The presence of hydroxyl molecules in the produced ZnONPs is indicated by a wideband at 3426.3 cm-1.(O-ZnO) after the removal of cefixime is displayed in Fig. (7). Vigorous stretching and the (O-ZnO) link are responsible for the peaks at (435.71 and 498.89135 cm−1), showing how the particles form. The band at (1031.04 cm-1) results from the existence of an amide group in the peel nanoparticles, but a deep and sharp band at (1629.71 cm−1) is caused by the presence of a water molecule (−OH) owing to C = O tiny peak (2923.5 cm−1)(Jabbar et al., 2023a). The presence of hydroxyl molecules in the produced (O-ZnO) is determined by a wideband at (3429.05 cm-1). Comparable Additional findings were acquired. by (Modi and Fulekar, 2020) and (Modi *et al.* 2022).

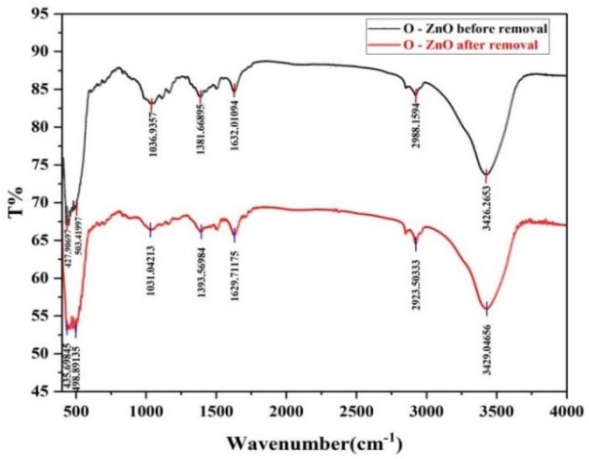

Fig. 7: FTIR spectra of (a) O-ZnO before removal and (b) O-ZnO after removal

3.1.4 Field-Emission Scanning Electron Microscopy (FE-SEM):

FESEM analysis of the synthesized ZnONps was carried out to determine the morphology of synthesized ZnO nanoparticles. For the FESEM studies, The shape and morphological features of the produced materials were examined using (FE-SEM), as shown in Fig.(8 a-c); the OPE surface

was consistent and showed that they have leaf-like structures with a size of 39.94 nm, as seen in Fig.(8-a). Several tiny cavities and holes were found. That indicated that OPE can be an excellent surface to synthesize ZnO nanoparticles.Fig.(8-b) shows the synthesized (O-ZnO). All the particles are spheroidal and submicron in size; however, they have merged to form a macroscopic structure that exceeds 100 nm in dimensions. At the same time, Photocatalytic activity caused the fusion of some nanoparticles. In actuality, the morphological attributes of the (O-ZnO)surface provide an advantage by increasing the available surface area for adsorption. Comparing Fig. (8-c) and the FESEM image after adsorption of (Cfx) in Fig. (8-c), It can be shown that during (Cfx) adsorption, (O-ZnO) morphological qualities were considerably altered. Because the pore surfaces were saturated with (Cfx) molecules, the surface of (O-ZnO)becomes brighter and smoother, and some previously separated agglomerates coalesce. Similar results were also reported by (Jan *et al.* 2021)**,** (Modi et al., 2022)**,** (Bekele et al., 2021)**,** (Xu and Xu, 2020)**.**

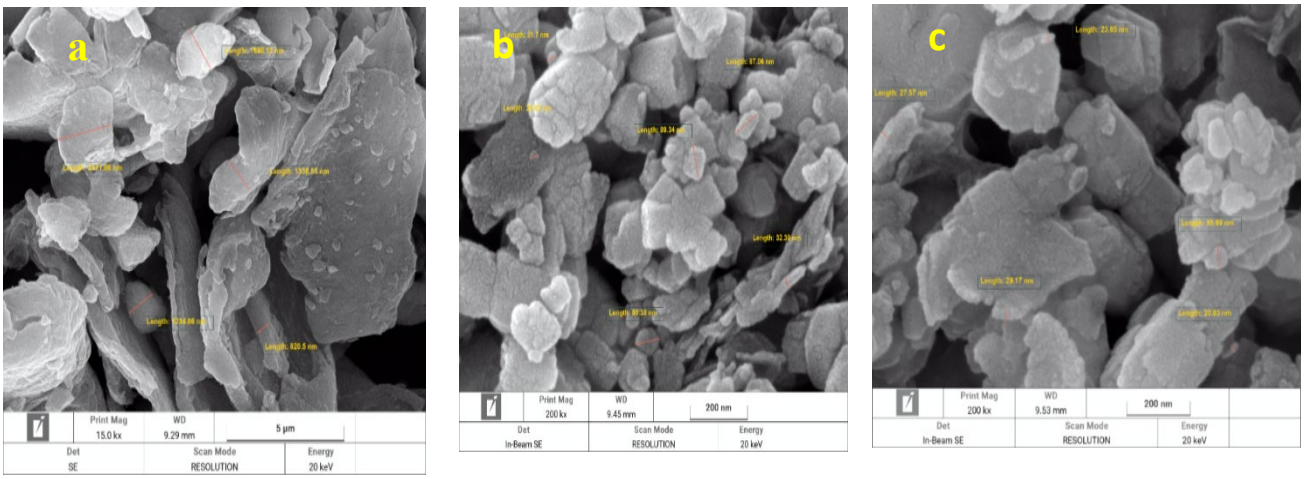

Fig. 8: FE-SEM images for (a) OPE, (b) (O-ZnO) before removal of Cfx, and (c) (O-ZnO) after removal of Cfx

3.2 BATCH EXPERIMENTS:

3.2.1 The impact of pH:

The initial pH of the solution is a crucial factor in photocatalytic processes, influencing the degradation and adsorption capacity of target organic compounds by modifying the photocatalyst's surface electrical charge properties and dictating the ionization state of the catalyst surface. The pH value affects the adsorption and dissociation capacity of chemicals, the charge distribution on the catalyst surface, and the oxidation potential of the catalyst's valence band. The pH of the solution varies with the degradation of pollutants; the pH impact was studied by shifting pH from an acid media (pH=2) to a basic medium (pH=10) as well as a neutral medium (pH=6). Fig.9 Hence, the

degradation of cefixime was studied under various pHs (Fig.9). From the results obtained, it was evident that the degradation catalyst, i.e., (O-ZnO), yielded a maximum degradation efficiency at pH = 4 (94%) and a similar degradation efficiency at pH = 3 (90%). When the pH was increased from 3 to 5, the degradation efficiency was increased; however, when pH was reduced from (7 to 10), they showed a relatively low effect on the degradation efficiency of cefixime. The variation in the degradation efficiency with varying pH could be attributed to the electrostatic interactions between (O-ZnO) charged particles and the contaminants. The pH of the solution had a significant role in determining the degree of dissociation of the pollutant. This point was related to the pKa value of the pollutant, which was considered to be 3 for cefixime. The acid-alkaline properties of the (O-ZnO) surface can have significant effects on their photocatalytic function.

3:2:2: The impact of dose:

The effect of catalyst dose on the photocatalytic degradation of cefixime using O-ZnO nanocomposite has been studied with nanocomposite concentrations varying from 0.1 to 0.6 g/100 ml (Fig.10). Results indicated that initially, with the increasing of nanocomposite concentration, the process efficiency of Cfx removal increased. The maximum removal was at the nanocomposite concentration of 0.4 g/100 mL. Still, with the increase of nanocomposite concentration to 0.6 g/100 mL of the nanocomposite, the degradation rate of contaminants exhibited a nearly linear trajectory, maybe attributable to the self-competitive interactions of the nanocomposite inside the solution. As the concentration became to 0.4 g/100 mL, the number of active sites on the nanocomposite surface, the generation of hydroxyl radicals, and the subsequent removal of Cfx escalated, contingent upon the catalyst surface sites and the intensity of UV radiation. Therefore, the catalyst concentration of 0.4g/100 L was chosen as the optimal Concentration for the next experiments in the study of photocatalytic Cfx removal utilizing O-ZnO nanocomposite (Derakhshani et al., 2023).

3:2:3: The impact of initial concentration:

Following the identification of the optimal solution pH, the findings from the analysis of antibiotic concentration effects are illustrated in Fig. (11). To enhance the elimination of cefixime by (O-ZnO), four additional doses of Cfx were tested alongside the standard concentration of 10 mg/L to identify the optimal concentration for degradation (El-Nahhas et al. 1992). The experiment results (Fig. 11) indicate that an increase in the initial Cfx concentration to 10 mg/L enhances degradation. Nevertheless, once the concentration above 20 mg/L, the degradation efficiency diminished, exhibiting a reduction of over 10%. The reduction may result from the influence of Cfx and intermediate metabolites on the photocatalytic reaction during degradation, including by the adsorption of UV light. The greatest degradation occurred at a concentration of 10 mg/L; the primary nanocomposite at the ideal pH demonstrated satisfactory effectiveness in removing Cfx within the 10 mg/L concentration range. (Semeraro et al. 2020).

3.2.4: The impact of contact time:

Contact time was an important factor that played a vital role in ensuring maximum efficiency of the photodegradation of the contaminant. In order to ascertain the optimum contact time for our catalyst, i.e., (O-ZnO), the degradation percentage for the contaminant was studied. A sample was collected at different time intervals in order to study the degradation percentage (Fig. 12). From the results obtained, we concluded that the removal trend for cefixime by the O-ZnO nanocomposite increases at 30 minutes and then gradually increases. The removal trend increased at 120 minutes, where the removal rate reached its peak and began to take a straight line at minute 180it. It was then observed that no further degradation took place. Therefore, the best time for the removal of cefixime by the O-ZnO nanocomposite, based on the following experiments, is 120 minutes. Hence, it can be said that initially, cefixime was oxidized rapidly by the generated radicals; however, with time, due to the formation of intermediates, the radicals generated were consumed, and the degradation efficiency was reduced (Ahmed et al. 2024).

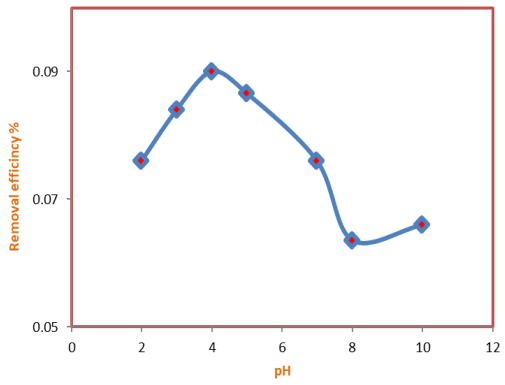

Fig. 9: Effect of pH on the degradation of (Cfx)

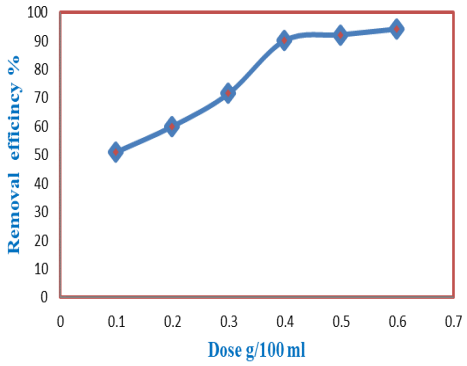

Fig.10: Effect of Dose on the degradation of (Cfx)

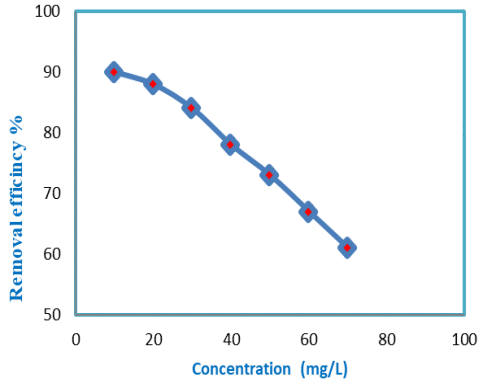

Fig. 11: Effect of Concentration on the degradation of (Cfx)

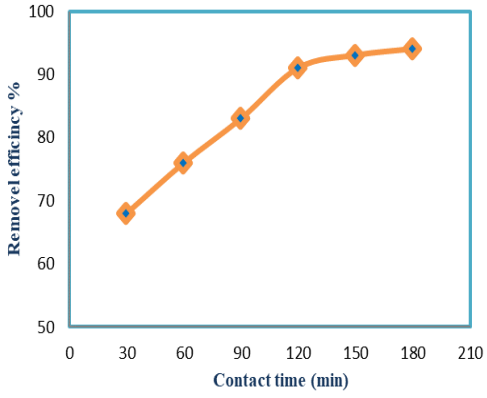

Fig. 12: Effect of time on the degradation of (Cfx)

3.4 KINETIC STUDY:

The kinetics of the photocatalytic reaction for Cfx degradation was examined based on the optimal conditions established in the preceding section (Ahmed et al. 2024). The kinetic models of

the pseudo-first-order reaction (Equation 1) and pseudo-second-order reaction (Equation 2) were used for studying 10 mg/l of Cfx residues removal from aqueous solution at pH =4 and O-ZnO= 0.4 mg/l; their results are shown in Table 5. The results revealed that the pseudo-kinematics of the first order showed the best correlation coefficient (R2= 0.9682) shown in Fig (13-a) and Fig (13-b). The final summarised version of this model is:

$$ln\frac{Co}{C} = K \qquad (1)$$

$$\frac{1}{C} - \frac{1}{Co} = Kt \qquad (2)$$

where k is the reaction's rate constant, C and C_o represent the Cfx concentrations (mg/l) following exposure time t and the initial Cfx concentration (mg/l), respectively, and t is the exposure duration (min).

Table 5: Reaction rate constants in heterogeneous photocatalysts.

First order		Second order	
K(min^{-1})	R^2	K(min^{-1})	R^2
0.0099	0.9682	0.0175	0.9186

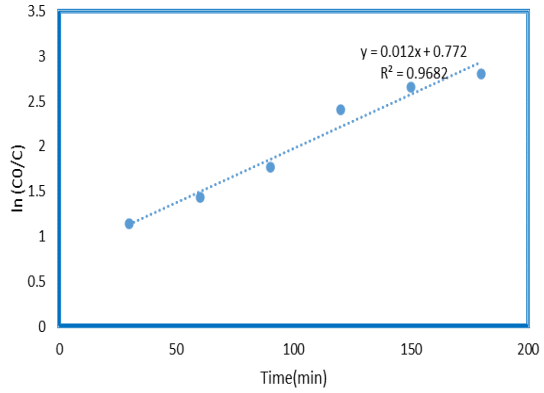

Fig.13-a – Kinetic study(first_order) of Cfx degradation based on optimum conditions

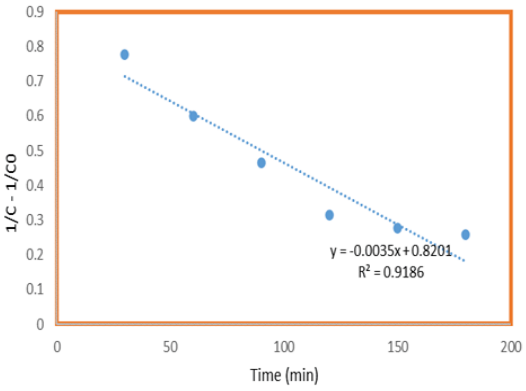

Fig. 13-b – Kinetic study(second_order) of Cfx degradation based on optimum conditions.

Table 6: A summary shows a comparison between previous studies on the preparation of ZnO for Cfx removal.

Composite	Pollutant	Efficiency (%)	Reference
(ZnO/GO/DES)	Cfx	86%	(Ciğeroğlu et al., 2022)

SWCNT/ZnO/Fe3O4	Cfx	94.19%.	(Erim et al., 2022)
ZnO/Fe3O4@MWCNTs	Cfx	90%	(Paidar et al., 2024)
O-ZnO	Cfx	94%	This Study

CONCLUSION:

Zinc oxide synthesis nanocomposite (O-ZnO) was performed. Onion peels extract were carried out for green synthesizing methods, while photocatalytic was selected from (AOP) synthesis methods. ZnO without (OPE) was used as a salt precursor. In contrast, onion peels extracts were utilized as agents for reduction for green synthesizing methods. (O-ZnO) was characterized by various techniques, including Fourier transform infrared (FT-IR), X-ray diffraction (XRD), scanning electron microscopy (SEM), Brunauer–Emmett–Teller (BET), and Barrentt-Joyner-Halenda (BJH). The activities of prepared nanopcompisite (O-ZnO) were evaluated on antibiotic cefixime. The crystal dimensions of the synthesized materials were determined using the Scherrer equation (21.7nm) for green synthesis nanocomposite (O-ZnO). Minor clusters were detected. from FESEM results of prepared (O-ZnO), OPE, (O-ZnO) after removal (Cfx). Prepared (O-ZnO) showed strong properties. These materials' morphology showed that the nanocomposite's size varied between 20–80 nm. In conclusion, this study revealed that 94% of the maximum removal efficiency was achieved at 4 pH and a concentration of 10 mg/L O-ZnO, 120 min, respectively. The green synthesis O-ZnO nanocomposite displayed appealing photocatalytic efficiency in deleting Cefixime residues from aqueous solutions. The results validated the efficiency of O-ZnO as a catalyst in the UV photocatalysis method for removing Cfx from an aqueous solution. Hence, the (O_ZnO) nanocomposite could be used as a semiconductor photocatalyst and a safe, eco-friendly, low-cost, and effective way to remove organic pollutants from an aqueous solution.

- **Author contributions:** All authors contributed to the study conception and design. Nabaa A. Al-Wahab performed materials preparation and experiments. Results analysis and models were performed by Rasha A. Al-husseiny. The first draft of the manuscript was written by Rasha A. Al-husseiny and Nabaa A. Al-Wahab. All authors read and approved the final manuscript**.**

- **Funding :** The authors did not receive support from any organization for the submitted work.
- **Institutional Review Board Statement:** "Not applicable."
- **Informed Consent Statement:** "Not applicable."
- **Acknowledgments:** The authors would like to thank Al-Qasim Green University, the College of Biotechnology, and the College of Veterinary Medicine for their moral support.

- **Conflicts of Interest:** "The authors declare no conflicts of interest."

REFERENCES:

Abbes, N., Bekri, I., Cheng, M., Sejri, N., Cheikrouhou, M., Xu, J., 2022. Green Synthesis and Characterization of Zinc Oxide Nanoparticles Using Mulberry Fruit and Their Antioxidant Activity. Medziagotyra 28, 144–150. https://doi.org/10.5755/j02.ms.28314

Abdullah, A., Mutmainnah, M., Sangkal, A., Ismail, R., 2022. UV-Vis Spectrophotometric Method Validation of Cefixime in Phosphate Buffer. Lumbung Farm. J. Ilmu Kefarmasian 3, 144–147.

Ahmed, A. M., Kareem, S. L., 2024. Evaluation of the effectiveness of phytoremediation technologies utilizing *Lemna minor* in constructed wetlands for wastewater treatment. *Biomass Conversion and Biorefinery* 1, 1–13.

Ahmed, A. M., Kareem, S. L., 2024. Evaluating the role of hydraulic retention time (HRT) in pollutant removal efficiency using Arundo donax in vertical subsurface flow constructed wetlands. Bioremediation Journal 1, 1–15.

Ajiwokewu, B.M., 2024. DEVELOPMENT OF TIO2/NH2-MIL-125 NANOCOMPOSITE FOR THE REMOVAL OF CIPROFLOXACIN UNDER INDUCED SOLAR IRRADIATION.

Al-husseiny, R.A., Ebrahim, S.E., 2022a. Effective Removal of Methylene Blue from Wastewater Using Magnetite / Geopolymer Composite : Synthesis , Characterization and Column Adsorption Study. Inorg. Chem. Commun. 139, 109318. https://doi.org/10.1016/j.inoche.2022.109318

Al-husseiny, R.A., Ebrahim, S.E., 2022b. construction. Environ. Nanotechnology, Monit. Manag. 18, 100700. https://doi.org/https://doi.org/10.1016/j.enmm.2022.100700

Al-husseiny, R.A., Ebrahim, S.E., 2021. Synthesis of geopolymer for the removal of hazardous waste : a review. https://doi.org/10.1088/1755-1315/779/1/012102

Al-husseiny, R.A., Kareem, S.L., Naje, A.S., Ebrahim, S.E., 2023. Effect of green synthesis of Fe3O4 nanomaterial on the removal of cefixime from aqueous solution. Biomass Convers. Biorefinery 1–12.

Bekele, B., Degefa, A., Tesgera, F., Jule, L.T., Shanmugam, R., Priyanka Dwarampudi, L., Nagaprasad, N., Ramasamy, K., 2021. Green versus chemical precipitation methods of preparing zinc oxide nanoparticles and investigation of antimicrobial properties. J. Nanomater. 2021, 1–10.

Ciğeroğlu, Z., Şahin, S., Kazan, E.S., 2022. One-pot green preparation of deep eutectic solvent-assisted ZnO/GO nanocomposite for cefixime trihydrate photocatalytic degradation under UV-A irradiation. Biomass Convers. Biorefinery 12, 73–86.

Derakhshani, E., Naghizadeh, A., Mortazavi-Derazkola, S., 2023. Biosynthesis of MnFe2O4@ TiO2 magnetic nanocomposite using oleaster tree bark for efficient photocatalytic degradation of humic acid in aqueous solutions. Environ. Sci. Pollut. Res. 30, 3862–3871.

Drummer, S., Madzimbamuto, T., Chowdhury, M., 2021. Green synthesis of transition-metal

nanoparticles and their oxides: A review. Materials (Basel). 14, 2700.

Erim, B., Ciğeroğlu, Z., Şahin, S., Vasseghian, Y., 2022. Photocatalytic degradation of cefixime in aqueous solutions using functionalized SWCNT/ZnO/Fe3O4 under UV-A irradiation. Chemosphere 291, 132929.

Haroon, K., Kherb, J., Jeyaseelan, C., Sen, M., 2023. Recent Advances and Sustainable Approaches Towards Efficient Wastewater Treatment Using Natural Waste Derived Nanocomposites: A Review. Nat. Environ. Pollut. Technol. 22.

Harouni, S., Bouanimba, N., Boulares, N., 2019. Synthesis of ZnO Nanostructures Using Sublimation-Condensation and Sol-Gel Methods: Evaluation of the Photocatalytic Degradation Activity of Industrial Dye. Acta Phys. Pol. A 136.

Hidayah, E.N., Cahyonugroho, O.H., Fauziyah, N.A., 2023. Performance of Alum Coagulation and Adsorption on Removing Organic Matter and E. coli. Nat. Environ. Pollut. Technol. 22, 497–502.

Jabbar, Z.H., Graimed, B.H., Okab, A.A., Alsunbuli, M.M., Al-husseiny, R.A., 2023a. Synthesis of geopolymer for the removal of hazardous waste: a review. J. Photochem. Photobiol. A Chem. 441, 114734. https://doi.org/10.1016/j.jphotochem.2023.114734

Jabbar, Z.H., Okab, A.A., Graimed, B.H., Issa, M.A., Ammar, S.H., 2023b. Photocatalytic destruction of Congo red dye in wastewater using a novel Ag2WO4/Bi2S3 nanocomposite decorated g-C3N4 nanosheet as ternary S-scheme heterojunction: Improving the charge transfer efficiency. Diam. Relat. Mater. 133, 109711.

Jan, H., Shah, M., Andleeb, A., Faisal, S., Khattak, A., Rizwan, M., Drouet, S., Hano, C., Abbasi, B.H., 2021. Plant-based synthesis of zinc oxide nanoparticles (ZnO-NPs) using aqueous leaf extract of aquilegia pubiflora: Their antiproliferative activity against HepG2 cells inducing reactive oxygen species and other in vitro properties. Oxid. Med. Cell. Longev. 2021.

Modi, S., Fulekar, M.H., 2020. Green synthesis of zinc oxide nanoparticles using garlic skin extract and its characterization. J. Nanostruct 10, 20–27.

Modi, S., Yadav, V.K., Choudhary, N., Alswieleh, A.M., Sharma, A.K., Bhardwaj, A., Khan, S.H., Yadav, K.K., Cheon, J.K., Jeon, B.H., 2022. Onion Peel Waste Mediated-Green Synthesis of Zinc Oxide Nanoparticles and Their Phytotoxicity on Mung Bean and Wheat Plant Growth. Materials (Basel). 15. https://doi.org/10.3390/ma15072393

Moosavi, F., Cheng, C., Gheinani, T., Traore, M., Kanaev, A., Nikravech, M., D'anna, A., Ciambelli, P., Sunseri, C., Gheinani, T.T., 2019. Photocatalytic Destruction of Amoxicillin in a Pilot Sunlight Reactor With Supported Titania Nano-Photocatalyst. https://doi.org/10.3303/CET1973030ï

Nagore, P., Ghotekar, S., Mane, K., Ghoti, A., Bilal, M., Roy, A., 2021. Structural properties and antimicrobial activities of Polyalthia longifolia leaf extract-mediated CuO nanoparticles. Bionanoscience 11, 579–589.

Paidar, R., Badalians Gholikandi, G., Alighardashi, A., Dadban shahamat, Y., Rahimzadeh Barzaki, H., 2024. Bio-ZnO/Fe3O4@ MWCNTs Magnetic Nanocomposites Promoted Green Synthesis of Pyrrole Derivatives and Removal of Cefixime and Amoxiciline from Aqueous Solution. Polycycl. Aromat. Compd. 44, 1991–2007.

Raina, S., Roy, A., Bharadvaja, N., 2020. Degradation of dyes using biologically synthesized silver and copper nanoparticles. Environ. Nanotechnology, Monit. Manag. 13, 100278.

Ramesh, P., Saravanan, K., Manogar, P., Johnson, J., Vinoth, E., Mayakannan, M., 2021. Green synthesis and characterization of biocompatible zinc oxide nanoparticles and evaluation of its antibacterial potential. Sens. Bio-Sensing Res. 31, 100399.

Roy, A., Singh, V., Sharma, S., Ali, D., Azad, A.K., Kumar, G., Emran, T. Bin, 2022. Antibacterial and dye degradation activity of green synthesized iron nanoparticles. J. Nanomater. 2022, 1–6.

Siripireddy, B., Mandal, B.K., 2017. Facile green synthesis of zinc oxide nanoparticles by Eucalyptus globulus and their photocatalytic and antioxidant activity. Adv. Powder Technol. 28, 785–797.

Widyasari, E.M., Hudriyah, A.N., Nuraeni, W., Wibawa, T.H.A., Sriyani, M.E., 2022. Physicochemical characteristic of 99mTc-DTPA-deoxy-D-glucose radiopharmaceutical, in: AIP Conference Proceedings. AIP Publishing.

Xu, H., Xu, L., 2020. Preparation of ZnO Nanomaterials and Their Photocatalytic Degradation of Organic Pollutants. J. Donghua Univ. Eng. Ed 37, 271–279.

El-Nahhas, F., El-Kadi, F., Ahmed, A., 1992. Interaction of tunnel linings and soft ground. Tunnelling and Underground Space Technology 7(1), 33–43.